(19) Casey, K.; Elston, C. T.; Phibbs, M. K. *Polym. Lett.* **1964**, *2*, 1053–1056.
(20) Tirpak, G. *Polym. Lett.* **1965**, *3*, 371–374.
(21) Tirpak, G. *Polym. Lett.* **1966**, *4*, 111–114.
(22) Van Dohlen, W. C.; Wilson, T. P. *J. Polym. Sci., Polym. Chem. Ed.* **1979**, *17*, 2511–2527.
(23) Van der Molen, Th. J. *Prepr. IUPAC Conf. (Budapest)* **1969**, *3*, 19.
(24) The following abbreviations are used in the remainder of the paper: $3MC_5$ = 3-methylpentane, $3MC_9$ = 3-methylnonane, $5MC_9$ = 5-methylnonane, etc. These are also used in the chromatograms.

Statistical Mechanical Theory of Deformation of Liquid Crystalline Structure in Styrene–Butadiene Diblock Copolymers in *n*-Tetradecane

Hiroshi Watanabe and Tadao Kotaka*

Faculty of Science, Department of Macromolecular Science, Osaka University, Toyonaka, Osaka 560, Japan. *Received September 15, 1982*

ABSTRACT: When a styrene–butadiene (SB) diblock copolymer is dissolved in a selective solvent such as *n*-tetradecane, which is a good solvent for the B blocks but a nonsolvent for the S blocks, micelles with S cores and B cilia are formed in the system. When the concentration and temperature are above and below the respective critical values, these micelles are arranged on a macrolattice to form a liquid crystalline structure, which exhibits plasticity. The rigidity of the macrolattice before yielding is calculated by a modified diffusion equation, as a result of inhomogeneity in concentration of ciliary B segments in the matrix phase induced by deformation of the macrolattice. When the SB concentration is high, the observed rigidity is proportional to the concentration. On the other hand, when the system is diluted, the observed rigidity is no longer proportional to the concentration but decreases more rapidly. The latter behavior is well simulated by the modified diffusion equation. The temperature dependence of the lattice rigidity is also discussed. The actual SB micelle systems exhibit thermally induced disordering of the macrolattice. However, our calculation assumes a narrow-interphase approximation and cannot predict this transition. A more realistic and complicated calculation is neccesary for the simulation of this thermal transition.

I. Introduction

Solutions of AB-type diblock copolymers in selective solvents, which dissolve only one of the two blocks but precipitate the other, often show peculiar rheology:[1-4] Plastic flow and thixotropy in steady shear flow[1-3] and nonlinear dynamic response due to the plasticity under oscillatory shear strain.[4,5]

In recent studies,[5-7] we examined the rheology of solutions of styrene–butadiene (SB) diblock copolymers dissolved in *n*-tetradecane (C14) and pointed out that the existence of higher order structure or liquid crystalline structure in the solution caused the plasticity and, hence, was responsible for the peculiar rheology. Since the solvent, C14, was a good solvent for the B block but a nonsolvent for the S block, microphase separation occurred and micelles with precipitated rigid S cores and dissolved B cilica were formed in the C14 solution. We call such an SB/C14 solution a "micelle system" in the following discussion. When the SB concentration c exceeded a certain critical concentration c_R^* and/or the temperature T was below a certain critical temperature T^*, the SB/C14 solution exhibited plasticity. However, the plasticity disappeared and the system became viscoelastic when c was below c_R^* and T was above T^*. Of course, c_R^* was dependent on T and T^* was dependent on c. These results[5-7] suggest that the formation of micelles in the solution is not enough but some higher order structure is required so that the micelle system exhibits plasticity.

Detailed small-angle X-ray scattering (SAXS) studies[6-8] revealed that in SB/C14 solutions below c_R^* and above T^*, where the solution is viscoelastic, micelles of SB molecules are randomly dispersed in the solution. In those above c_R^* and below T^*, where the system exhibits plasticity, these micelles are arranged on a simple cubic (sc) type lattice[6-8] (but *not* on a face centered cubic (fcc) type lattice, which had been assumed to exist). We call this lattice a "macrolattice" in the following discussion.

To describe the morphology of microdomain structure of block copolymers in bulk, where the compressibility is low and inhomogeneous density profiles of the block segments in each domain are strongly inhibited, Meier[9] and Helfand and co-workers[10-12] developed a mean field theory and solved modified diffusion equations under the incompressible limit. Helfand and co-workers[11,12] treated this situation by introducing a potential term that depended on the square of the density deviation divided by the (infinitely) small compressibility into the diffusion equation. As the result, the size and morphology (spherical, cylindrical, or lamellar structure) of the microdomains were determined as a function of composition and molecular weight in such a way that each block chain confined in a microdomain can assume the thermodynamically most stable (optimal) conformation, avoiding those conformations that create density inhomogeneity in the microdomain. They could successfully predict the domain size and shape and the interphase structure.[9-12] Their theoretical predictions were substantiated by Hashimoto and coworkers[13] in their SAXS studies. However, for systems having spherical domains Meier[9] and Helfand and Wasserman[12] employed a spherically symmetric geometry to describe each domain and did not determine what type of packing of the spherical domains would be the most stable one.

Recently, Noolandi and Hong[14] extended the modified diffusion equation approach to block copolymer solutions, taking into account solvent–polymer interactions explicitly. They solved the mean field equation under the constraint of no volume change upon mixing solvent molecules and block segments for lamellar block copolymer structure and investigated the effect of solvent on the size and interphase structure of the microdomains. For the SB/toluene system, in which toluene is a common good solvent for both

0024-9297/83/2216-1783$01.50/0

S and B blocks, they found a first-order "melting" transition for the periodic lamellar structure when the SB block copolymer became saturated with toluene.[14]

In SB/C14 systems in the present study,[6,7] the S blocks (swollen with a small amount of solvent) formed rigid spherical cores of the micelles and the ciliary B blocks dissolved in C14 formed the matrix phase. Above c_R^* and below T^* such micelles were arranged on a macrolattice of sc type.[6-8] When the magnitude of applied stress was small enough, the system did not flow but responded as if a linear elastic body.[4-6] In such a system inhomogeneity in the overall density generated by imposing a small strain would be automatically compensated by freely mobile solvent molecules. The S core phase would be also incompressible and undeformable as long as the stress is small. However, there remains an inhomogeneity of local concentration of dissolved B segments in the matrix phase. Such concentration inhomogeneity could be supplemented by conformational changes in B cilia as well as opposed by an osmotic pressure gradient generated in the matrix phase of the distorted macrolattice. Unlike a bulk system having very low compressibility, such a solution has a rather high osmotic compressibility as long as the concentration is not too high. Thus, the macrolattice seems to be stabilized under the conditions such that the dissolved B segments occupy the matrix phase as uniformly as possible, and at the same time, the conformation of the B blocks is that having maximum conformational entropy.

We attempted to simulate the rheology of such a macrolattice system with a modified diffusion equation similar in nature to those of Meier[8] and Helfand.[9-12] On the basis of SAXS data on the morphology of SB/C14 solutions,[5-7] we formulated the diffusion equation for ciliary B chains with one end of each chain being fixed on the surface of the rigid S core and the whole micelle being confined in a cubic cell of the macrolattice. The modified diffusion equation was solved numerically to calculate the free energy difference between the unstrained and strained macrolattice as the results of conformational changes of the B cilia and gradient in the concentration profile of the B segments in the matrix phase induced by the shear strain. Thus, the rigidity of the macrolattice before yielding was calculated. The calculated rigidity of the macrolattice as a function of SB concentration was compared with the experimental results on SB/C14 solutions.

II. Theory

1. Modified Diffusion Equation. For calculating the rigidity of the sc-type macrolattice on which the micelles with spherical S cores and dissolved B cilica are arranged, the free energy of the system must be estimated as a function of strain γ imposed on the system. A periodic cell is used in such calculations because of the symmetry of the macrolattice. Specifically, we employed a cubic cell shown in Figure 1. The three axes x, y, z of the cubic cell coincide with the three directions x', y', z' of the translational symmetry of the macrolattice when no strain is imposed. On the other hand, when a strain γ is imposed and affine deformation is assumed, the macrolattice becomes a monoclinic lattice instead of the simple cubic one at $\gamma = 0$. Then, the y' axis of the deformed macrolattice deviates from the spatially fixed y axis of the cell.

A modified diffusion equation[9-12] eq 1 is given as

$$\frac{\partial}{\partial t} Q(\mathbf{r},t;\mathbf{r}_0) = \left[\frac{b^2}{6}\nabla^2 - u(\mathbf{r}) \right] Q(\mathbf{r},t;\mathbf{r}_0) \qquad (1)$$

where b denotes the segment step length. The function $Q(\mathbf{r},t;\mathbf{r}_0)$ is proportional to the probability density that a chain with number of segments t has one end at $\mathbf{r}_0$ and the other at $\mathbf{r}$.[11] Equation 1 describes the conformation of a polymer chain affected by the potential term $u(\mathbf{r})$. The strain γ determines the cell symmetry and affects the solution $Q(\mathbf{r},t;\mathbf{r}_0)$ of eq 1 through the boundary conditions.

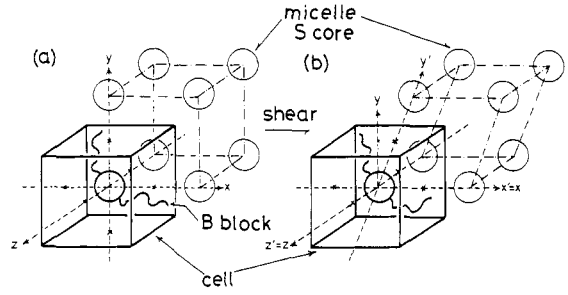

Figure 1. Schematic diagram representing the cubic cell used in the calculation of the rigidity of the macrolattice. Note that the three axes x, y, z of the cell are spatially fixed and deviate from the three directions x', y', z' of the translational symmetry of the macrolattice when a shear is imposed.

Strictly speaking, eq 1 must be solved for both the S and B blocks in the SB micelle system. In our micelle systems, however, the strain seems to affect little the S core and the interphase between the S core and dissolved B phase (matrix phase), because the matrix phase is a solution of the B block and much softer than the S cores. Therefore, in our semiempirical approach to calculate the change in the free energy density of the deformed and undeformed macrolattice, we solve eq 1 only for the dissolved B blocks assuming that the S phase is a rigid core of radius d_S (found by SAXS). For simplicity, we further assume that one end of the B block is fixed on the surface of the S core and the S core is an inhibited region for the B blocks, i.e., the narrow-interphase approximation.[12]

To solve the modified diffusion equation eq 1, the potential term $u(\mathbf{r})$ should be written explicitly. In block copolymer solutions, the gradient in the overall (solvent + block segments) density is strongly inhibited. However, the gradient in the copolymer segment concentration would emerge by rather small energy. Hong and Noolandi[14] employed the condition of constant overall density as a Lagrangian multiplier in their derivation of the potential term. Therefore, their potential term written in terms of the chemical potential and interactions among the solvent molecules and copolymer segments did not include the compressibility explicitly.[14]

In principle, all of the following factors affecting the conformation of the dissolved block, the interaction of the blocks with solvents, the combinatorial entropy of the solvent molecules, the interfacial energy, the loss of entropy due to localization of the block copolymer joints, the change of conformational entropy due to stretching and collapsing of the blocks, and the osmotic effect, i.e., the demand of uniform concentration profile of the B-block segments in the matrix phase, should be incorporated in the potential term. However, to examine the stability of the macrolattice with known shape and dimensions under the assumptions mentioned above, we may neglect in this primary calculation all these factors except the osmotic effect. This assumption may be justified by the experimental results[15] that the macrolattice loses its stability and becomes disordered when the solvent C14 is replaced by homopolybutadiene (hB). The hB dissolves only B blocks, and micelles with S cores and B cilia are formed in SB/hB systems. Since hB molecules are chemically identical with the B blocks but are freely mobile in the matrix phase, they act as a buffer for the inhomogeneity of the B-segment concentration. That is, the demand of uniform concen-

tration profile of the B segments is always satisfied by hB molecules, and this demand due to the osmotic effect cannot affect the conformation of the B blocks in SB/hB systems. On the other hand, all of the other factors described above would not change much even when C14 is replaced by hB. Thus, the osmotic effect would be the most dominant factor that affects the conformation of the B blocks and stabilizes the macrolattice in SB/C14 solutions.

Such an effect of the concentration inhomogeneity on the stability of the macrolattice in SB/C14 solutions may be expressed in a most straightforward manner by introducing the osmotic compressibility explicitly in the calculation. As described later, the magnitude of the osmotic effect rapidly decreases as the (osmotic) compressibility increases rapidly with decreasing concentration. Thus, in the following calculations, we assume a potential term similar to that of Helfand and co-workers[11] for bulk block copolymers instead of the complete one for the solution described by Hong and Noolandi.[14]

According to Helfand and co-workers,[11] the potential term $u(\mathbf{r})$ is determined from the free energy density of mixing $\Delta f(\mathbf{r})$ as

$$\Delta f(\mathbf{r}) = \frac{(\tilde{\rho}(\mathbf{r}) - 1)^2}{2\kappa} \tag{2}$$

$$u(\mathbf{r}) = \frac{1}{kT}\frac{\partial \Delta f}{\partial \rho} = \frac{\tilde{\rho}(\mathbf{r}) - 1}{\kappa k T \rho_0} \tag{3}$$

$$\tilde{\rho}(\mathbf{r}) = \rho(\mathbf{r})/\rho_0 \tag{4}$$

where $\rho(\mathbf{r})$ is the number density of B-block segments at $\mathbf{r}$, ρ_0 the mean value of $\rho(\mathbf{r})$ in the matrix phase, $\tilde{\rho}(\mathbf{r})$ the reduced number density at $\mathbf{r}$, k the Boltzmann constant, T the temperature, and κ the compressibility. The potential term $u(\mathbf{r})$ acts so that the demand of uniformly filling the space becomes satisfied.

The segment density $\rho(\mathbf{r})$ is given by $Q(\mathbf{r},t;\mathbf{r}_0)$ as

$$\rho(\mathbf{r}) = \frac{N_m}{Q^* V}\int_0^{n_B} dt \int^{\text{cell}} d\mathbf{r}' \int^{\text{boundary}} d\mathbf{r}_b\, Q(\mathbf{r},t;\mathbf{r}_b) Q(\mathbf{r}',n_B-t;\mathbf{r}) \tag{5}$$

$$Q^* = \frac{1}{V}\int^{\text{cell}} d\mathbf{r}' \int^{\text{boundary}} d\mathbf{r}_b\, Q(\mathbf{r}',n_B;\mathbf{r}_b) \tag{6}$$

where N_m is the number of SB molecules per micelle, n_B the number of segments per B block, and V the volume of the matrix phase in the cell. The normalization condition for $\rho(\mathbf{r})$ is given as

$$\int^{\text{cell}} \rho(\mathbf{r})\, d\mathbf{r} = n_B N_m \tag{7}$$

The integral $\int^{\text{boundary}}...d\mathbf{r}'$ is carried out in the boundary region, which is a thin spherical shell surrounding the S core. The potential term $u(\mathbf{r})$ in eq 1 is determined by $Q(\mathbf{r},t;\mathbf{r}_0)$ through eq 2–6, and eq 1 is in turn a nonlinear equation for $Q(\mathbf{r},t;\mathbf{r}_0)$. Numerical calculations are required to solve eq 1. The initial conditions for $Q(\mathbf{r},t;\mathbf{r}_0)$ is given as

$$Q(\mathbf{r},0;\mathbf{r}_0) = \delta(\mathbf{r} - \mathbf{r}_0) \tag{8}$$

where $\delta(\mathbf{r} - \mathbf{r}_0)$ is the Dirac δ function. After a consistent set of $\rho(\mathbf{r})$, $u(\mathbf{r})$, and $Q(\mathbf{r},t;\mathbf{r}_0)$ is obtained, the free energy density F of the micelle system is calculated as[11,12]

$$F = -\frac{kTN_m}{D^3}\ln Q^* + \frac{1}{D^3}\int^{\text{cell}}\left[\Delta f - \rho\frac{\partial \Delta f}{\partial \rho}\right] d\mathbf{r} \tag{9}$$

where D denotes the cell constant, being equal to the spacing of the macrolattice. After the free energy density F is calculated for a given γ, the change in F is differentiated twice to give the rigidity G of the macrolattice as

$$\Delta F = F|_{\gamma=\gamma} - F|_{\gamma=0} \tag{10}$$

$$G = \partial^2 \Delta F/\partial \gamma^2 \tag{11}$$

In the actual calculations some modifications were made. To save the computation time and memory space of the electronic computer employed, we reduced the function $Q(\mathbf{r},t;\mathbf{r}_0)$ to two functions $q_B(\mathbf{r},t)$ and $q_C(\mathbf{r},t)$, defined as

$$q_B(\mathbf{r},t) = \int^{\text{boundary}} d\mathbf{r}_b\, Q(\mathbf{r},t;\mathbf{r}_b) \tag{12a}$$

$$q_C(\mathbf{r},t) = \int^{\text{cell}} d\mathbf{r}'\, Q(\mathbf{r}',t;\mathbf{r}) \tag{12b}$$

Both $q_B(\mathbf{r},t)$ and $q_C(\mathbf{r},t)$ statisfy the modified diffusion equation as

$$\frac{\partial}{\partial t} q_i(\mathbf{r},t) = \left[\frac{b^2}{6}\nabla^2 - u(\mathbf{r})\right] q_i(\mathbf{r},t), \qquad i = \text{B, C} \tag{1'}$$

From $q_B(\mathbf{r},t)$ and $q_C(\mathbf{r},t)$, the segment density $\rho(\mathbf{r})$ is calculated as

$$\rho(\mathbf{r}) = \frac{N_m}{Q^* V}\int_0^{n_B} dt\, q_B(\mathbf{r},t) q_C(\mathbf{r},n_B-t) \tag{5'}$$

$$Q^* = \frac{1}{V}\int^{\text{cell}} d\mathbf{r}\, q_B(\mathbf{r},n_B) = \frac{1}{V}\int^{\text{boundary}} d\mathbf{r}_b\, q_C(\mathbf{r}_b,n_B) \tag{6'}$$

As the boundary condition, $q_B(\mathbf{r},t)$ and $q_C(\mathbf{r},t)$ have the translational symmetry along the axes x', y', z' of the macrolattice (see Figure 1). Besides this, eq 13 is employed as the boundary condition[16] because the S domain is the inhibited region for the B blocks.

$$q_B(\mathbf{r},t) = 0 \quad \text{in the boundary region and S domain } (t > 0) \tag{13a}$$

$$q_C(\mathbf{r},t) = 0 \quad \text{in the S domain } (t > 0) \tag{13b}$$

On the other hand, the initial conditions are given as

$$q_B(\mathbf{r},0) = 1 \quad \text{in the boundary region}; \quad = 0 \quad \text{otherwise} \tag{8'a}$$

$$q_C(\mathbf{r},0) = 0 \quad \text{in the S core}; \quad = 1 \quad \text{otherwise} \tag{8'b}$$

Some comments must be made here about the difficulties of the calculation for SB solutions. The theory of Meier[9] and Helfand and co-workers[10–12] treated the incompressible limit, i.e., $\kappa = 0$. Then the potential term $u(\mathbf{r})$ in eq 1 and 1′ becomes unknown and an adjustable function. On the other hand, in our micelle systems, a gradient or inhomogeneity of the concentration of B segments in the matrix phase is not completely inhibited and $\kappa \neq 0$. This condition $\kappa \neq 0$ requires the actual calculation for $u(\mathbf{r})$, which must be consistent with $q_B(\mathbf{r},t)$ and $q_C(\mathbf{r},t)$ in eq 1′. Then the elegant technique incorporating an adjustable $u(\mathbf{r})$ used by Helfand and Wasserman[12] cannot be applied to our problem. Furthermore, we treat the deformed macrolattice where the three axes x, y, z of the cubic cell are not identical with each other. Because of these points, we had to carry out numerical calculations in a time-consuming manner. A few methods such as a perturbation calculation with a Green function and an eigenvalue expansion method were examined. However, these calculations were not convergent. The most suc-

cessful method examined was a simple numerical differentiation method, and we employed this one. The details of the calculation are described in the Appendix.

2. Estimation of Compressibility κ and Step Length b. As described in the previous section, the value of the compressibility κ must be known in our calculation. Since the thermodynamic force acting in our micelle system is attributed to the local inhomogeneity of the B-segment concentration c, κ can be estimated from the osmotic pressure Π as

$$\kappa = -c\frac{\partial(1/c)}{\partial \Pi} \tag{14}$$

For homopolymer solutions, the critical threshold[17] c^* is given as

$$c^* \cong \left(\frac{4\pi}{3}\right)^{-1} \langle s^2 \rangle^{-3/2} M N_A^{-1} \quad \text{(g of polymer)/cm}^3 \tag{15}$$

where $\langle s^2 \rangle$ is the mean square radius of gyration and M the molecular weight of the polymer chain. In semidilute solution,[17] i.e., $c > c^*$, the osmotic pressure depends on c as[18,19]

$$\frac{\Pi M}{cRT} = K'\left(\frac{c^*}{c}\right)^{1/(3\nu-1)} \tag{16}$$

where K' is a constant of about 1.50, and ν is an exponent factor of about 0.585, given as[19]

$$\langle s^2 \rangle \propto M^{2\nu} \qquad \text{(in good solvent)} \tag{17}$$

Since our B block has an anchored end, application of eq 16 is a little problematic. In this connection, the concentration seems to fluctuate in the scale of our interest, and strictly speaking, κ is not a constant but depends on the position in the cell. For simplicity, however, all of these factors were neglected, and κ in our calculation was estimated from eq 14–16, where M was replaced by the molecular weight of the B blocks.

We must also estimate the value of the step length b. In a bulk state, the chains are in the Θ state. On the other hand, in our SB/C14 micelle systems, the dissolved B blocks seem to be moderately expanded because the solvent C14 is good for B blocks and the solution is in a semidilute state. Equation 1 does not incorporate this excluded volume effect and some modification is required. For this purpose, we simply employed the *blob model*[17] and regarded the expanded B block consisting of n_B monomers as an ideal chain consisting of Z blobs. The blob size ξ and the number g of B monomers per blob are given as[17]

$$\xi \cong b_K \phi^{-3/4} \tag{18a}$$

$$g \cong \phi^{-5/4} \tag{18b}$$

where b_K is the Kuhn step length of polybutadiene homopolymer in the bulk state, and ϕ the volume fraction of B segments in the matrix phase. Therefore, we replaced n_B and b in eq 1–13 by $Z = n_B/g$ and ξ in eq 18a, respectively, and employed the values of Z and ξ in the actual calculations.

III. Results and Discussion

1. Quantitative Comparison between the Observed and Calculated Rigidity. We have already carried out dynamic measurements for 10 wt % C14 solutions of five SB diblock copolymers with narrow molecular weight distributions.[7] When the stress was kept smaller than the yield value, these solutions exhibited almost elastic behavior with small loss of mechanical energy.[7] Simulations for these systems were carried out. However, the convergence was rather poor for those with long B blocks and a concentrated matrix phase. In this section, we make a simulation for the 10 wt % C14 solution of SB1 copolymer ($M_n = 66 \times 10^3$, PS content = 29.3 wt %),[7] having the shortest B block and the largest PS content among the five copolymers examined. The rigidity before yielding observed for this system at 25 °C is about 2.8×10^3 dyn cm^{-2}.[7]

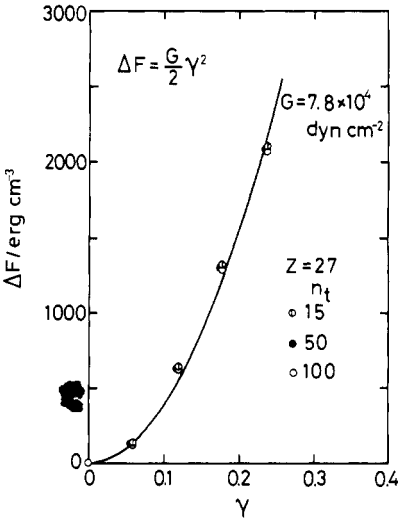

Figure 2. Strain γ dependence of the free energy density increment ΔF calculated for the 10 wt % SB1/C14 solution at 25 °C.

Figure 2 shows the γ dependence of the free energy density increment ΔF calculated for the 10 wt % SB1/C14 solution at 25 °C by eq 10. The parameters used in this calculation were estimated from the molecular weight and PS content of SB1, the concentration of the solution, and previously obtained SAXS data on the sizes of the S core and macrolattice.[7] The compressibility κ, the number Z of blobs per B block, the number g of B monomers per blob, and the step length ξ of the blob were estimated from eq 14–18 as

$$\kappa = 6.9 \times 10^{-7} \text{ dyn}^{-1} \text{ cm}^2, \qquad Z = 27, \qquad g = 31.9, \qquad \xi = 50 \text{ Å} \tag{19}$$

It should be emphasized here that our calculation includes no adjustable parameters. To examine the accuracy of the numerical differentiation $\partial/\partial t$, each blob was further divided equally into n_t pieces and therefore each B block into Zn_t pieces in the calculation. Three values of n_t, 15, 50, and 100, were examined. On the other hand, the cubic cell was divided equally into $17 \times 17 \times 17 = 4913$ pieces. As shown in Figure 2, the calculated values of ΔF for $n_t = 15$, 50, and 100 were in good agreement, exhibiting a good convergence of the numerical calculation. The calculated ΔF is approximately a quadratic function of the strain γ as represented by the solid curve in the figure. The increase in ΔF corresponds to the breakdown of the cell symmetry. Figure 3 shows the concentration profiles on the three axes x', y', z' of the macrolattice calculated for $n_t = 100$. When $\gamma = 0$ (Figure 3a), the three axes are identical with each other. An imposition of the strain breaks this symmetry, and the profiles on the three axes become different from each other (Figure 3b). We also notice another point in Figure 3a as follows: When we compare the profiles of $\tilde{\rho}$ calculated for the potential term $u = (\tilde{\rho} - 1)/(\kappa k T \rho_0)$ and $u = 0$, the deviation of $\tilde{\rho}$ from the mean value $\tilde{\rho} = 1$ is smaller in the former. This result shows that the potential term $u = (\tilde{\rho} - 1)/(\kappa k T \rho_0)$ acts to diminish the concentration inhomogeneity.

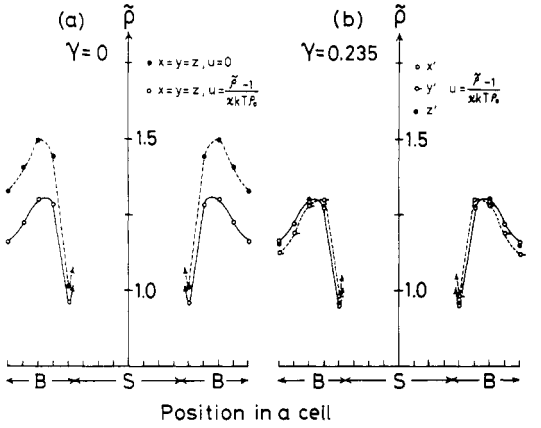

Figure 3. Concentration profile calculated for the 10 wt % SB1/C14 solution at 25 °C on the three axes x', y', z' of the macrolattice.

From the results shown in Figure 2, the rigidity of the macrolattice is calculated from eq 11 as

$$G = 7.8 \times 10^4 \text{ dyn cm}^{-2} \qquad (20)$$

The calculated value is about 30 times larger than the observed one, 2.8×10^3 dyn cm^{-2}. The difference between them may be attributed to dislocations[20] in the macrolattice. Our calculation employs the periodic cubic cell and therefore assumes a perfect crystal structure. However, there must exist many dislocations in the macrolattice of the SB micelles. For many metals, theoretical estimates of the elastic limit of perfect crystals give values 100 or more times higher than observed ones because of dislocations existing in actual crystals. If we assume the same situation in our comparison of the observed and calculated rigidity of the macrolattice, their ratio of about 30 is rather small and the agreement is fairly good. This result suggests that the modified diffusion equation incorporating the potential term due to the segment concentration inhomogeneity in the matrix phase simulates the rheology of the macrolattice, at least semiquantitatively.

2. Concentration Dependence of the Rigidity of the Macrolattice. In a previous paper of the present authors and the Kyoto University group,[21] we reported the concentration dependence of the rigidity of C14 solutions of a commerical SB sample (coded as cSB; Solprene 1205, Phillips Petroleum, $M_n = 52 \times 10^3$, PS content = 29.5 wt %). A simulation was carried out for the behavior of cSB/C14 solutions with the modified diffusion equation. The parameters used in the calculation were estimated in a manner similar to that described in the previous section. When the concentration of the cSB/C14 system is high, the convergence of the calculation becomes poor because of the difficulty in calculating $\tilde{p}$ for small κ. Therefore, we carried out the simulation for the system having relatively low concentrations.

Figure 4 shows (a) the concentration profile calculated for $\gamma = 0$ and (b) the γ dependence of the ΔF. The results (i), (ii), and (iii) in the figure correspond to cSB/C14 solutions with the concentration of 5, 10, and 20 wt %, respectively. The compressibility κ becomes smaller with increasing concentration, and the concentration profile becomes more uniform as shown in Figure 4a. Corresponding to this result, the ΔF increases more rapidly with increasing γ when the system becomes concentrated (Figure 4b). The γ dependence of the ΔF is approximated by a quadratic function, and the rigidity G is calculated as indicated in the figure.

Figure 5 compares the observed[21] and calculated rigidity as a function of the volume fraction ϕ of the B segments

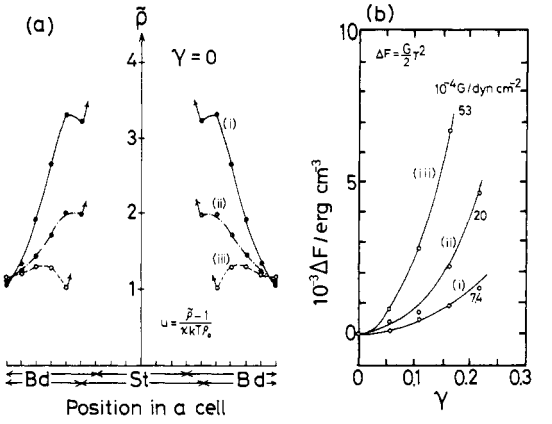

Figure 4. Results of the calculations for the cSB/C14 solutions with concentrations of (i) 5, (ii) 10, and (iii) 20 wt % at 25 °C: (a) concentration profile calculated for $\gamma = 0$; (b) strain γ dependence of the free energy density increment ΔF.

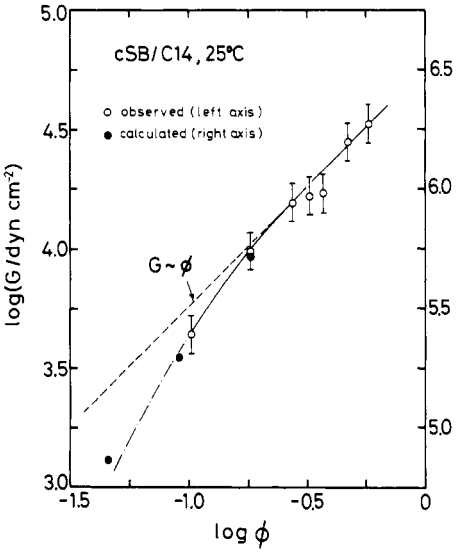

Figure 5. Comparison of the concentration dependence of the observed (open circles) and calculated (filled circles) rigidity of the cSB/C14 solutions.

in the matrix phase for cSB/C14 micelle systems at 25 °C. As described in the previous section, the calculated value is larger than the observed one, presumably because of dislocations in the macrolattice. We simply reduce the calculated value by a factor $10^{-1.75} \cong 1/56$ and compare its ϕ dependence with the observed results. When ϕ is large, the observed rigidity (open circles) becomes proportional to ϕ. This result is interpreted as follows:[21] In concentrated systems, the concentration profile is almost uniform because of very small κ, and only the change in the constraint entropy[9,12] ΔS_{const} induced by the strain contributes to the free energy density increment ΔF. The loss of entropy per B block caused by the strain becomes independent of ϕ when ϕ is large enough and the compressibility κ is small enough. Then ΔS_{const} becomes simply proportional to the number of B blocks per unit volume and therefore proportional to ϕ. This leads to the linear relationships $\Delta F \propto \phi$ and $G \propto \phi$. However, when ϕ becomes small, the observed rigidity is not proportional to ϕ but decreases more rapidly. The calculated result (filled circles) well simulates this rapidly decreasing behavior. This result suggests that the contribution of ΔS_{const} to ΔF is small, but the concentration inhomogeneity induced by the strain is the main factor contributing to the increase in the free energy density when ϕ is small and κ is large.

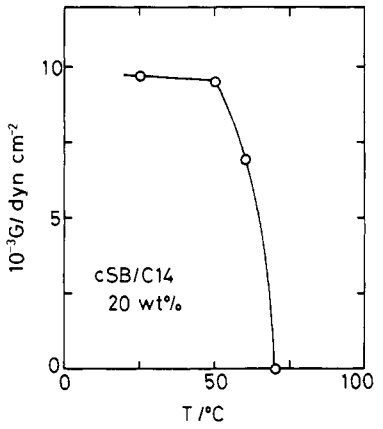

Figure 6. Temperature dependence of the observed rigidity of the 20 wt % cSB/C14 solution.

3. Temperature Dependence of the Rigidity of the Macrolattice. Figure 6 shows the temperature dependence of the observed rigidity for 20 wt % cSB/C14 solution.[6] The system loses its plasticity at about 70 °C, which we call the critical temperature T^*. This transition of rheology corresponds to disordering of the macrolattice, and the micelles themselves are still preserved as long as the temperature T is not very high.[6] The transition shows that the driving force for the macrolattice formation suddenly vanishes when $T > T^*$. However, in our calculation, such a drastic change cannot be simulated. Since the osmotic pressure Π is proportional to T as shown in eq 16, the compressibility κ is proportional to T^{-1} and the potential term $u = (\tilde{p} - 1)/(\kappa k T \rho_0)$ is independent of T. This shows the calculated rigidity is independent of T.

This peculiar result that our calculation cannot explain the effect of temperature on rheology may be interpreted as follows: First, the narrow-interphase approximation employed in our calculation becomes invalid when the temperature is high. Although the micelles themselves are still preserved when $T \gtrsim T^*$, a mixing of the S and B blocks must occur to some extent to make the interphase more diffuse. Secondly, the temperature dependence of κ may be somewhat different from that shown in eq 14 and 16 because eq 16 is the relationship for solutions of homopolymer chains in good solvents. Our preliminary experiments[7] suggest that the diffuse interphase plays a key role in the macrolattice disordering induced by a temperature rise. To simulate the T dependence of G, we must solve eq 1 for both the S and B blocks, allowing mixing of the two components. However, such calculations are highly complicated and have not yet been carried out.

Acknowledgment. We express heartfelt thanks to Professor Masao Doi, Tokyo Metropolitan University, who kindly suggested the boundary condition for the modified diffusion equation. We acknowledge with thanks the financial support from the Ministry of Education, Science, and Culture (Mombusho) under Grants 347081 and 543026. All the numerical calculations in this study were carried out at the Computation Center, Osaka University, with its ACOS Series 77, NEAC System 900 and 1000.

Appendix

In this appendix, the numerical method employed in the present study is briefly described. First, the variables $\mathbf{r} = (x,y,z)^+$ and t were divided equally as

$$x_i = x = (i - N - 1)\frac{D}{2N+1}$$
$$y_j = y = (j - N - 1)\frac{D}{2N+1}$$
$$z_k = z = (k - N - 1)\frac{D}{2N+1}$$
$$t_m = t = (m - 1)\frac{1}{n_t} \quad \text{(A-1)}$$
$$i, j, k = 1, ..., 2N+1; \qquad m = 1, ..., Zn_t + 1$$

where D is the experimentally determined spacing of the macrolattice and Z is the number of blobs per B block. Typically, $N \cong 10$, $Zn_t = 100$–300, and a few thousand kilowords of memory space in the electronic computer was required to carry out the calculation.

The functions $q_K(\mathbf{r},t)$ were written as $q_K(i,j,k,m)$ (K = B, C) and similarly $u(\mathbf{r})$ as $u(i,j,k)$. The modified diffusion equation was rewritten as

$$q_K(i,j,k,m) = q_K(i,j,k,m-1) + \frac{\xi^2(2N+1)^2}{6n_tD^2}[q_K(i+1,j,k,m-1) + q_K(i-1,j,k,m-1) + q_K(i,j+1,k,m-1) + q_K(i,j-1,k,m-1) + q_K(i,j,k+1,m-1) + q_K(i,j,k-1,m-1) - 6q_K(i,j,k,m-1)] - \frac{1}{n_t}u(i,j,k)q_K(i,j,k,m-1) \quad \text{(A-2)}$$

To determine $q_K(i,j,k,m)$ in a stepwise manner by eq A-2, the divided cell piece (i,j,k) was assigned as

if $(|x_i| - \delta)^2 + (|y_j| - \delta)^2 + (|z_k| - \delta)^2 < d_S^2$ (i,j,k) is in the S core

if $(|x_i| - \delta)^2 + (|y_j| - \delta)^2 + (|z_k| - \delta)^2 > d_S^2$ (i,j,k) is in the matrix phase

otherwise (i,j,k) is in the boundary region (A-3)

where $\delta = (1/2)[D/(2N+1)]$, and d_S is the experimentally determined radius of the S core. The numerical calculation started from the initial condition eq 8′ and the q_K at t_m was obtained from q_K at t_{m-1} and u by eq A-2. In the calculation, q_K sometimes became negative because the divided intervals of t and $\mathbf{r}$ were finite. At that time, q_K was set to be zero and the calculation was continued. As the boundary condition, $q_B(i,j,k,m)$ is set to be zero for $m \geq 2$ (cf. eq 13) in the boundary region. The value of $q_C(i,j,k,m)$ in the boundary region was also necessary in the calculation of q_C by eq A-2. For this purpose, an additional condition eq A-4 was employed.

$$q_C(i,j,k,m) = \sum_{\substack{(i',j',k') \\ \text{in the cell}}} q_B(i',j',k',m) \Big/ \sum_{\substack{(i',j',k') \text{ in} \\ \text{the boundary} \\ \text{region}}} \quad \text{(A-4)}$$

We assumed that q_C was constant in the boundary region, and eq A-4 was derived from the definitions of q_B and q_C given in eq 12. Besides, q_B and q_C were always set to be zero in the S core, because the S core was the inhibited region for the B blocks.

When $i+1, j+1, k+1 \geq 2N+1$ or $i-1, j-1, k-1 \leq 0$ in eq A-2, the translational symmetry of q_K was utilized as

$$q_K(\mathbf{r}+\mathbf{a}_1+\mathbf{a}_2+\mathbf{a}_3,t) = q_K(\mathbf{r},t) \quad \text{(A-5)}$$

where $\mathbf{a}_1$, $\mathbf{a}_2$, and $\mathbf{a}_3$ represent the three translational vectors along the axes x', y', z' of the macrolattice (see Figure 1). The strain γ imposed on the system determines these vectors and affects q_K and therefore also affects the

free energy of the system. That is, eq A-5 is the boundary condition that represents the effect of γ. After $q_B(i,j,k,m)$ and $q_C(i,j,k,m)$ were obtained, $\rho(i,j,k)$ ($=\rho(\mathbf{r})$) was calculated by eq 5′ and 6′. Then the normalization condition for $\rho(i,j,k)$, eq 7, was employed, and $\rho(i,j,k)$ was adjusted by a factor

$$n_B N_m (2N+1)^3/D^3 \sum_{\substack{(i,j,k) \text{ in} \\ \text{the matrix} \\ \text{phase}}} \rho(i,j,k)$$

because q_K is proportional to but not identical with the probability density.

The actual process of obtaining a consistent set of q_K and ρ was as follows: First, eq A-2 was solved for $u = 0$ and the trial functions of q_K and q_C were obtained for a given γ by the procedure described above. Then ρ was calculated from these q_B and q_C, and the first trial potential term $u(i,j,k)$ was calculated from this ρ by eq 2–4. Then eq A-2 was solved for this $u(i,j,k)$ and the same steps were repeated until the calculation became convergent. This procedure is similar to the perturbation calculation where the potential term u acts as an internal disturbance. Thus, the calculation was convergent when the disturbance u was not very large; i.e., the osmotic compressibility introduced in this term was not very small. When the mean change of $\rho(i,j,k)$ in the cell and the change of Q^* (see eq 6′) in the subsequent step became smaller than a suitably chosen criterion, say 0.2% of the whole value in this study, the calculation for that γ was terminated, and a new loop for another γ was initiated. Such a calculation sometimes took 2 h or more for five values of γ.

References and Notes

(1) Kotaka, T.; White, J. L. *Trans. Soc. Rheol.* **1973**, *17*, 587.
(2) Masuda, T.; Matsumoto, Y.; Matsumoto, T.; Onogi, S. *Nihon Reoroji Gakkaishi* **1977**, *5*, 135. Masuda, T.; Matsumoto, Y.; Onogi, S. *J. Macromol. Sci., Phys.* **1980**, *B17*, 256.
(3) Osaki, K.; Kim, B. S.; Kurata, M. *Bull. Inst. Chem. Res., Kyoto Univ.* **1978**, *56*, 56.
(4) Watanabe, H.; Kotaka, T. *Nihon Reoroji Gakkaishi* **1980**, *8*, 26.
(5) Kotaka, T.; Watanabe, H. *Nihon Reoroji Gakkaishi* **1982**, *10*, 24. Kotaka, T.; Watanabe, H. *Polym. Eng. Rev.*, in press.
(6) Watanabe, H.; Kotaka, T.; Hashimoto, T.; Shibayama, M.; Kawai, H. *J. Rheol.* **1982**, *26*, 153.
(7) Watanabe, H.; Kotaka, T. *Polym. J.* **1982**, *14*, 739. The SB samples employed were those with S content less than 30 wt % and molecular weight M_n less than 3×10^5.
(8) Shibayama, M.; Hashimoto, T.; Kawai, H. *Macromolecules* **1983**, *16*, 16.
(9) Meier, D. J. *J. Polym. Sci., Part C* **1969**, *26*, 81. Meier, D. J. *Prepr. Polym. Colloq., Soc. Polym. Sci. Jpn.* **1977**, *1*, 83.
(10) Helfand, E.; Tagami, Y. *J. Chem. Phys.* **1972**, *56*, 3592. Helfand, E.; Sapse, A. M. *Ibid.* **1975**, *62*, 1327.
(11) Helfand, E. *J. Chem. Phys.* **1975**, *62*, 999. Helfand, E. *Acc. Chem. Res.* **1975**, *8*, 295. Helfand, E. *Macrmolecules* **1975**, *8*, 552.
(12) Helfand, E.; Wasserman, Z. R. *Macromolecules* **1976**, *9*, 879. Helfand, E.; Wasserman, Z. R. *Polym. Eng. Sci.* **1977**, *17*, 582. Helfand, E.; Wasserman, Z. R. *Macromolecules* **1978**, *11*, 960.
(13) Hashimoto, T.; Todo, A.; Itoi, H.; Kawai, H. *Macromolecules* **1977**, *10*, 377. Hashimoto, T.; Shibayama, M.; Kawai, H. *Ibid.* **1980**, *13*, 1237.
(14) Noolandi, J.; Hong, K. M. *Ferroelectrics* **1983**, *30*, 117. Hong, K. M.; Noolandi, J. *Macromolecules* **1981**, *14*, 727. Hong, K. M.; Noolandi, J. *Ibid.* **1981**, *14*, 736.
(15) Watanabe, H.; Kotaka, T. *J. Rheol.* **1983**, *27*, 223. Watanabe, H.; Kotaka, T. *Macromolecules* **1983**, *16*, 769.
(16) Doi, M., private communication.
(17) See, for example: de Gennes, P.-G. "Scaling Concepts in Polymer Physics"; Cornell University Press: Ithaca, NY, 1979.
(18) des Cloizeaux, J. *J. Phys. (Paris)* **1975**, *36*, 281.
(19) Noda, I.; Kato, N.; Kitano, T.; Nagasawa, M. *Macromolecules* **1981**, *14*, 668.
(20) Kittel, C. "Introduction to Solid State Physics", 5th ed.; Wiley: New York, 1976.
(21) Shibayama, M.; Hashimoto, T.; Kawai, H.; Watanabe, H.; Kotaka, T. *Macromolecules* **1983**, *16*, 361.

Long-Range Order Parameters of Form II of Poly(vinylidene fluoride) and Molecular Motion in the α_c Relaxation

Yasuhiro Takahashi* and Kazuhiro Miyaji

Faculty of Science, Department of Macromolecular Science, Osaka University, Toyonaka, Osaka 560, Japan.

Received January 25, 1983

ABSTRACT: Long-range order parameters S_A and S_C are defined as linear functions of the structure factor ratios of superlattice spots 120 and 031 to the standard reflection 130, respectively. The reflection intensities of 120, 031, and 130 were measured over the temperature range 55–170 °C by a position-sensitive proportional counter system. The parameter S_A is independent of temperature, while the parameter S_C decreases with increasing temperature. This suggests that the reverse motion, which changes the molecular orientation along the fiber axis, takes place in a crystallite. The temperature range corresponds to the α_c relaxation that is observed, and the reverse motion is essentially the same as that proposed by Miyamoto et al.[6] for the molecular motion in the α_c relaxation.

The α relaxation is observed at the highest temperature and the lowest frequency by dielectric measurements of form II of poly(vinylidene fluoride). It was established by several authors[1-3] that the α relaxation is caused by molecular motion in the crystalline region of form II. Nakagawa and Ishida[4] attributed the α relaxation to the coupled motion of chain loops at the crystalline surface and chain rotation with a small lengthwise translation in the interior of the crystal. McBrierty et al.[5] interpreted the NMR data by two models: rotation of crystalline chains in the vicinity of defects and rotational oscillation of restricted amplitude of all chains about the chain axis. Miyamoto et al.[6] proposed a mechanism in which the reverse of the molecular orientation along the fiber axis takes place during movement of a defect region, and Clark et al.[7] characterized the defect region as a solitary wave.

In a previous paper,[8] it was established that in form II crystal, four molecules with different orientation statistically occupy a crystal site with different existence probabilities (Figure 1). The analysis suggests that re-

0024-9297/83/2216-1789$01.50/0